Hindawi
Mathematical Problems in Engineering
Volume 2019, Article ID 5261869, 11 pages
https://doi.org/10.1155/2019/5261869

Research Article

Energy-Saving Design of Building Envelope Based on Multiparameter Optimization

Weinan Gan,[1] Yunzhong Cao,[1] Wen Jiang,[1] Liangqiang Li,[2] and Xiaolin Li[2]

[1]*College of Architecture and Urban-Rural Planning, Sichuan Agricultural University, Chengdu 611830, China*
[2]*Business School, Sichuan Agricultural University, Chengdu 611830, China*

Correspondence should be addressed to Yunzhong Cao; caoyz@sicau.edu.cn and Wen Jiang; xuezhongsha_wen@163.com

Received 25 July 2019; Accepted 18 November 2019; Published 10 December 2019

Academic Editor: Denizar Cruz Martins

The contradiction between the indoor environment and building energy consumption has been controversial. The design of building envelope involves many parameters such as window size and exterior wall material. These parameters have significant influence on building energy-saving design and indoor environment. In this paper, nondominant sorting genetic algorithm-II (NSGA-II) is utilized to calculate winter heat consumption, indoor total lighting energy consumption, and thermal comfort. The Pareto method is used to select the compromise solution and effective value of each building parameter. Different from other studies, we add more architectural design variables into the model calculation, which can bring architects more detailed energy-saving design content.

1. Introduction

With global energy shortages, many countries have adopted corresponding energy policies, and global energy intensity declined by 1.8 percent in 2016, based on primary energy demand for gross domestic product (GDP). China's energy intensity has declined sharply, reflecting the continuing impact on energy efficiency policies [1]. But, the final energy consumption of buildings rose steadily from 119EJ in 2010 to 124EJ in 2016, at a rate that went beyond reduction in energy intensity. Along with the advancement of China's urbanization process, more than 97% of new buildings each year are high energy-consuming buildings, and the total energy consumption of buildings accounts for about 30% of the total energy consumption of Chinese society. China's building energy consumption accounts for about 6.0% of global energy consumption, equal to the total energy consumption in the Middle East, twice that of Africa and twice that of Japan and South Korea combined [2]. In China, urban buildings are mainly divided into residential buildings and nonresidential buildings. Nonresidential buildings (public buildings) such as government buildings, commercial buildings, and school buildings account for a large proportion of building energy consumption, and the comprehensive energy consumption per square meter is more than twice that of residential buildings [3]. Therefore, energy conservation in public buildings is of great significance.

The highest potential for green building energy-saving design lies in the renovation of building envelope structures to reduce the use of air conditioning system. Effective design scheme can not only respond to the needs of green energy-saving and long-term economic benefits brought by government investment but also meet the user's comfort level. Through the local climatic conditions and site conditions, architects can maximize the control of architectural design and construction techniques [4]. Building envelope parameters can affect building energy performance and comfort to a considerable extent. Building envelope is usually composed of transparent and opaque components, and the solar energy and shading characteristics transmitted by materials' heat conduction,

windows, and the total projection rate of composite materials affect the cooling and heating load of buildings and energy consumption of lighting system [5, 6].The geometric configurations of buildings, such as the building volume, the aspect ratio of windows, and the window wall ratio [7, 8], are counted as additional factors influencing the energy load of buildings.

In this article, indoor thermal performance, thermal comfort, and lighting energy consumption of NSGA-II are optimized by building geometry and physical boundary. Building energy consumption, indoor basic thermal comfort, and indoor use lighting are the three objectives of this study. The value range of each building parameter (design variable) is taken according to the national standard specification. The Pareto method selects the optimal solution set, and the different nondominated solutions correspond to discrete building parameters.

2. The Mathematical Model

We have built three objective functions. The first objective function (f_1) includes the winter heat consumption of the enclosure and the summer cooling load. We use the heat consumption Q as the positive here. Therefore, to calculate their total energy consumption, we must subtract. The second (f_2) is to calculate the total lighting energy consumption f_2 for the whole year, and finally we use the PMV (predicted average voting) value f_3 to analyze the thermal comfort of the room in summer. The design variables of these three objective functions have some coupling. It can be seen from the model of the objective function later. For example, the window design in f_2 also affects f_1. And f_1 and f_3 also have contradictory relations. More design variables help to provide a richer context for the architect, which is the novelty of this article. The model created in this article does not limit the maximum or minimum of the solution goal. This is to get more solutions. This solution set is more flexible and diverse. The final choice will be decided by the architect.

$$\begin{cases} f_1 = -q_{\text{sys}} + Q, \\ f_2 = E_{\text{el}}, \\ f_3 = \text{PMV}. \end{cases} \tag{1}$$

2.1. Lighting Energy Consumption. The assumption of diffuse reflection lighting conditions leads to another metric commonly referred to as the daylight factor (DF) [9], which is the ratio of indoor and outdoor illumination under standard CIE cloudy conditions. Due to the simplified sky model, given a certain daylight open configuration, regardless of direction, geographic location, and climate change, the DF at a particular point will remain approximately constant; for the purpose of design, the vector flux splitting method [10] is used. The DF consists of three separate components: sky (SC), external reflection (ERC), and internal reflection (IRC) components:

$$\text{DF} = (\text{SC} + \text{ERC} + \text{IRC}). \tag{2}$$

About complex design calculations, ERC can be determined by multiplying the external obstacle (SC_{obs}, i.e., obstacles can be seen in the sky area) by the obstacle reflectivity (R_{obs}, this paper takes a value of 0.2), and the calculation for IRC is also taken from [11]:

$$\text{IRC} = \frac{\tau_j A_j}{A(1-R)}\left(CR_{\text{fw}} + 5R_{\text{cw}}\right). \tag{3}$$

In order to achieve a more practical design, additional calibration was performed in this paper, taking into account the maintenance factor (M_{f}), glass factor (G), and window frame factor (B), with values of 0.9, 1, and 0.85 [12], respectively. The final calculated DF is

$$\text{DF} = 0.765\,(\text{SC} + \text{ERC} + 0.2\text{SC}). \tag{4}$$

For the case where the calculation point is close enough to daylight, SC can be considered as the most important component of the three. SC is pure geometric calculation as shown in Figure 1. The calculation equation of SC is as follows:.

$$\begin{aligned} \text{SC} = \frac{E_{i,\text{sky}}}{E_O} &= \frac{(L_z/3)\int_0^{\theta'}\int_0^{\beta}(1+2\sin\theta)\sin\theta\cos\theta\,d\theta\,d\psi}{(L_z/3)\int_0^{2\pi}\int_0^{\pi/2}(1+2\sin\theta)\sin\theta\cos\theta\,d\theta\,d\psi} \\ &= \frac{3}{14\pi}\left(\beta - \beta'\cos\gamma\right) + \frac{2}{7\pi}\arcsin\left(\sin\beta\sin\gamma\right) \\ &\quad - \frac{1}{7\pi}\left(\sin 2\gamma\sin\beta'\right). \end{aligned}$$

Known :

$$\begin{aligned} \tan\theta' &= \tan\gamma\cos\psi, \\ \tan\beta &= \frac{L}{D}, \\ \tan\beta' &= \tan\beta\cos\gamma = \frac{L/D}{\sqrt{(H/D)^2 + 1}}. \end{aligned} \tag{5}$$

In the lighting design, there are roughly two possibilities for the position of the window relative to the calculation point; this paper refers to the position of the calculation point by Mangkuto [14]. The projection of the calculation point is located in the window area and internal or external (Figure 2); the height of the working surface is 0.75 m and is higher than the window sill position. Let the distance from the observation point to the left wall be x, which is calculated as follows:

when $x \le D/2 - L_i/2$,

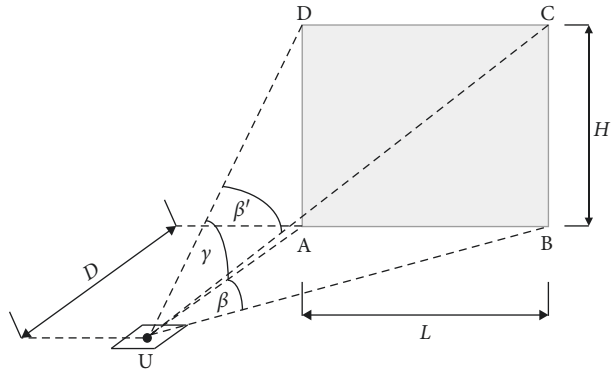

Figure 1: Diagram of the calculation of U from the vertical, effective daylight opening ABCD to D (from [13]).

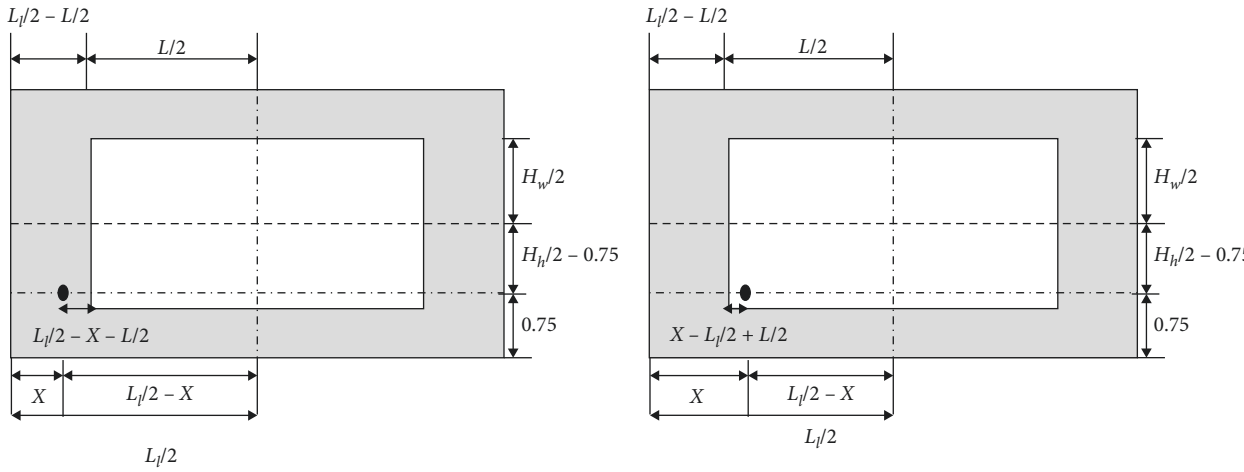

Figure 2: Sectional view of the window wall, two possibilities for the position of the window relative to the calculated point (m).

$$\mathrm{SC}_{(a)} = \mathrm{SC}\left(\frac{L}{D} = \frac{L_l - x + (L_i/2)}{d}, \frac{H}{D} = \frac{(H_h/2) - 0.75 + (H_j/2)}{d}\right) - \mathrm{SC}\left(\frac{L}{D} = \frac{L_l - x - (L_i/2)}{d}, \frac{H}{D} = \frac{(H_h/2) - 0.75 + (H_j/2)}{d}\right), \tag{6}$$

when $D/2 > x > D/2 - L_i/2$,

$$\mathrm{SC}_{(b)} = \mathrm{SC}\left(\frac{L}{D} = \frac{L_l - x + (L_i/2)}{d}, \frac{H}{D} = \frac{(H_h/2) - 0.75 + (H_j/2)}{d}\right) - \mathrm{SC}\left(\frac{L}{D} = \frac{L_l + (L_i/2)}{d}, \frac{H}{D} = \frac{(H_h/2) - 0.75 + (H_j/2)}{d}\right). \tag{7}$$

Annual lighting energy demand ($E_{\mathrm{el}}\mathrm{KWh/m^2/yr}$) refers to the total demand for electric lighting and energy lighting throughout the year. According to the national standard [15], the maximum value of the library building lighting power density limit target is 8 ($\mathrm{W/m^2}$), and each point of the illumination E_{in} is multiplied by the relevant DF multiplied by the outdoor diffuse, The selected value of the illuminance E_{out} is calculated. If the value of E_{in} is less than 300 lx (reading room illuminance standard value), then additional lighting is needed, and E_{in} at all points is averaged with a positive difference of 300 lx and multiplied by $\eta = 37.5$ lm/W (i.e. 300 lx per 8 $\mathrm{W/m^2}$) to obtain the desired illumination power density [14]. T is the total working time (8 hours/day × 5 days/week × 52 weeks/year), and we finally get the estimated E_{el}:

$$E_{\mathrm{el}}\left[\mathrm{KWh/m^2/yr}\right] = \frac{T}{1000m\eta}\sum_{i=1}^{m}\left(300 - E_{\mathrm{in},i}\right) = \frac{0.55}{m}\sum_{i=1}^{m}\left(300 - E_{\mathrm{in},i}\right). \tag{8}$$

2.2. Heat Consumption. The calculation of the basic heat consumption of the envelope structure refers to the

national standard [16]. The heat consumption of the external protection structure of the universal layer is mainly composed of the outer window and the outer wall. The outer wall is composed of a concrete wall, interface mortar (or bonding layer), insulation layer (or insulation board), crack protection layer (or plaster layer), and veneer layer.

The heat consumption of the enclosure consists of basic heat consumption (9) and additional heat consumption. The heat transfer coefficient is composed of the heat transfer coefficients of each structure, and their relationship is shown in formula (10). The additional heat consumption is determined as a percentage of the basic heat consumption. It mainly includes the orientation correction rate, the wind attachment rate, the external door attachment rate, the height addition rate of the building (except the stairwell), and the intermittent addition rate. The outdoor temperature air temperature is a harmonic time parameter with an angular frequency. Therefore, a simple prediction [17] can be performed using equation (10). The indoor air temperature is determined by the indoor setting temperature. And the interior design temperature is designed according to the level of thermal comfort, as can be seen from Table 1. The calculation method of the heat consumption of the envelope structure is shown in formula (11).

$$Q_0 = \alpha FK\left(t_{\mathrm{n}} - t_{\mathrm{wn}}\right), \tag{9}$$

$$K = \frac{1}{\left(1/a_{\mathrm{n}}\right) + \sum\left(\delta/a_{\lambda}\cdot\lambda\right) + R_k + \left(1/a_{\mathrm{w}}\right)}, \tag{10}$$

$$t_{\mathrm{wn}} = \widetilde{t_{\mathrm{wn}}} + \Delta t_{\mathrm{wn}}\sin\left(\omega t\right), \tag{11}$$

$$Q = \alpha FK\left(t_{\mathrm{n}} - t_{\mathrm{wn}}\right)\left(1 + \mathrm{or} + \mathrm{hh} + \mathrm{od}\right). \tag{12}$$

In formula (10), a_{n} represents the heat transfer coefficient of the inner surface of the envelope, a_{w} represents the heat transfer coefficient of the outer surface of the enclosure, and a_{λ} represents the correction coefficient of material thermal conductivity. Their values are shown in Tables 2 and 3, respectively [18].

2.3. Cooling Load. The heat transfer process of the building envelope is a very complex process involving convection, conduction, and radiation. At the same time, the outdoor air temperature and heat radiation density also change greatly with the change of outdoor time, and the indoor air temperature also changes. In this paper, the heat transfer equation of external thermal mass and internal air is used to calculate the hourly cooling load of the enclosure. The following assumptions are made:

(i) The air distribution within the building, the temperature distribution of the internal thermal mass, and the internal surface temperature of the external thermal mass are balanced.

(ii) All thermal gain and heat generation in the building are assembled into a heat source E during the working period, while there is no room thermal gain during the nonworking period, and the radiant heat exchange between the heat source and other surfaces is ignored.

(iii) The direct thermal solar radiation gain and permeability thermal gain through the opening were ignored.

(iv) During the nonworking period, the air conditioning system is closed and night ventilation mode is adopted. The ventilation rate is Q_{v}.

Based on the above assumptions, the heat balance equations of the inner surface temperature and the indoor air temperature of the outer envelope structure are as shown in equations (13) and (14) [17]:

$$\mathrm{MC_m}\frac{\partial T_{\mathrm{is}}}{\partial t} + h_0A_0\left(T_{\mathrm{is}} - T_0\right) + h_iA_0\left(T_{\mathrm{is}} - T_i\right) = 0, \tag{13}$$

$$q_{\mathrm{sys}} + h_iA_0\left(T_{\mathrm{is}} - T_i\right) + E = 0. \tag{14}$$

The calculation of outdoor air temperature in summer is similar to formula (11):

$$T_0 = \widetilde{T_0} + \Delta\widetilde{T_0}\sin\left(\omega t\right). \tag{15}$$

Substitute equation (15) into equation (13):

$$\mathrm{MC_m}\frac{\partial T_{is}}{\partial t} + \left(h_0 + h_i\right)A_0T_{is} = h_0A_0\widetilde{T_0} + h_iA_0T_i + h_0A_0\sin\left(\omega t\right). \tag{16}$$

Let $\tau = \mathrm{MC_m}/\rho C_{\mathrm{p}}Q_{\mathrm{v}}$, where τ is the time constant based on night ventilation rate Q_{v}; $\lambda_0 = h_0A_0/\rho C_{\mathrm{p}}Q_{\mathrm{v}}$, where λ_0 is the dimensionless external convective heat transfer; and $\lambda_i = h_{\mathrm{I}}A_0/\rho C_{\mathrm{p}}Q_{\mathrm{v}}$, where λ_i is the dimensionless internal convective heat transfer.

Substitute τ, λ_0, and λ_i into formula (16):

$$\omega\tau\frac{\partial T_{\mathrm{is}}}{\partial\left(\omega t\right)} + \left(\lambda_0 + \lambda_i\right)T_{\mathrm{is}} = \lambda_0\widetilde{T_0} + \lambda_iT_i + \lambda_0\Delta\widetilde{T_0}\sin\left(\omega t\right). \tag{17}$$

λ_0 and λ_i, respectively, measure the external and internal convective heat transfer intensities of the surface of the outer envelope. In buildings with large external or internal convection heat transfer, the efficiency of internal or external convection heat transfer is higher than that of indoor air mixing.

The general solution of equation (17) [17] is

$$T_{\mathrm{is}}\left(\omega t\right) = \frac{\lambda_0}{\lambda_0 + \lambda_{\mathrm{i}}}\widetilde{T_0} + \frac{\lambda_{\mathrm{i}}}{\lambda_0 + \lambda_{\mathrm{i}}}T_i + \frac{\lambda_{\mathrm{i}}\lambda_0}{\sqrt{\left(\lambda_0 + \lambda_{\mathrm{i}}\right)^2 + \omega^2\tau^2}}\Delta\widetilde{T_0} \cdot \sin\left(\omega t - \beta_1\right) + C_1\lambda_{\mathrm{i}}e^{-\left\{\left(\lambda_0+\lambda_{\mathrm{i}}\right)/\omega\tau\right\}\omega t}, \tag{18}$$

where C_1 is a constant and $\beta_1 = \tan^{-1}\left\{\omega\tau/\left(\lambda_0 + \lambda_{\mathrm{i}}\right)\right\}$ is the relative delay parameter of cooling load with respect to outdoor air temperature; it is evaluated from 0 to $\pi/2$.

Substitute equation (18) into equation (14) [17]:

Table 1: Indoor design temperature of air conditioning in the area where personnel stay for a long time t_n.

Working condition of the category	Thermal comfort level	Interior design temperature (°C)
Heating conditions	I level	22~24
	II level	18~22
Cooling conditions	I level	24~26
	II level	26~28

Table 2: Heat transfer coefficient of inner surface of envelope a_n.

Internal surface characteristics of envelope	$a_n[W/(m^2 \cdot K)]$
A wall, floor or ceiling with a flat surface or ribbed projection, $h/s \le 0.3$	8.7
A ribbed, well-shaped roof, $0.2 < h/s \le 0.3$	8.1
A ceiling with ribbed projections, $h/s > 0.3$	7.6
A roof with a well-shaped projection $h/s > 0.3$	7.0

Table 3: Heat transfer coefficient of outer surface of envelope a_w.

Outer surface characteristics of envelope	$a_w[W/(m^2 \cdot K)]$
Exterior walls and roof	23
A floor above an unheated basement that communicates with outdoor air	17
A floor slab above a nonheated basement with a covered roof and windows on the exterior wall	12
A windowless, unheated floor above a basement	6

$$q_{sys} = -\rho C_p Q_v \left\{ T_E + \frac{\lambda_i \lambda_0}{\lambda_0 + \lambda_i}\left(\widetilde{T}_0 - T_i\right) + \frac{\lambda_i \lambda_0}{\sqrt{(\lambda_0 + \lambda_i)^2 + \omega^2 \tau^2}} \cdot \Delta \widetilde{T}_0 \sin\left(\omega t - \beta_1\right) + C_1 \lambda_i e^{-\{(\lambda_0 + \lambda_i)/\omega\tau\}\omega t} \right\}. \tag{19}$$

In equation (18), q represents the cooling load that needs to meet the indoor hot air balance in summer and T represents the temperature rise caused by indoor heat source, $T_E = E/\rho C_p Q_v$. The cooling load is mainly composed of three parts. The first part is the steady-state cooling load, which is jointly caused by the steady-state heat source and the heat gain generated by the temperature difference between indoor and outdoor through the convective heat transfer of hot substances. The second part is the periodic fluctuation cooling load Δq_{sys}, whose amplitude depends on the fluctuation $\Delta \widetilde{T}_0$ of outdoor air temperature. The third part (exponential part) is caused by its initial conditions, which will decay to 0 with the increase of time and external convective heat transfer or the decrease of time constant.

2.4. Evaluation of Indoor Thermal Environment Model. PMV is the most comprehensive evaluation considering many factors of human thermal comfort. Table 4 shows the thermal and cold ruler of ASHRAE corresponding to PMV. ISO defines the thermal comfort range as $-0.5 \le \text{PMV} \le 0.5$. In order to reduce energy consumption of building air conditioning, China reduces the comfort range to $-1 \le \text{PMV} \le 1$.

There are coupling effects among various factors affecting thermal sensation, for example, the increase of temperature can be compensated by the decrease of humidity or the increase of wind speed. ASHRAE defines thermal comfort as a psychologically satisfying thermal environment, which mainly includes six major factors, namely, air temperature, average radiant temperature, relative humidity, air velocity, human metabolism, and clothing [17]. Due to the complexity of PMV calculation, it is not conducive to engineering practice. Therefore, this paper chooses a simple calculation method for thermal environment assessment proposed [19].

$$\text{PMV} = 2.43 - 3.67\text{HB}, \tag{20}$$

$$\text{HB} = \frac{\left(T_{sk} - T_{op}\right)}{M1\left(I_{cl} + I_a/f_{cl}\right)} = \frac{\left(T_{sk} - T_{op}\right)/\left(I_{cl} + I_a/f_{cl}\right)}{M1}. \tag{21}$$

The molecule of formula (21) represents heat loss through sensible heat of skin, and the denominator represents total heat production of human body. Since invisible latent heat is inevitable, the value of the fraction must be less than 1, and its value represents the ratio of sensible heat dissipation to total heat production [19]. T_{sk} represents the average skin temperature. Since the skin temperature is relatively constant, the change range is very small in an environment close to thermal comfort. Here, the average skin temperature in the thermal comfort state is calculated at 33.5°C.

According to ISO-7730 [20], when the wind speed is less than 0.2 m/s or the temperature difference between the average radiation temperature T_{mrt} and the air is less than 4°C, the calculation of the acting temperature T_{op} is as follows:

$$T_{op} = AT_i + (1 - A)T_{mrt},$$
$$A = \begin{cases} 0.5, & v < 0.2\ \text{m/s}, \\ 0.6, & 0.2\ \text{m/s} \le v < 0.6\ \text{m/s}, \\ 0.7, & 0.6\ \text{m/s} \le v < 1\ \text{m/s}. \end{cases} \tag{22}$$

I_{cl} represents thermal resistance of clothing. f_{cl} represents the clothing area coefficient, and its calculation method is shown in (23). I_a represents the thermal resistance of air outside the garment, which is a function of air temperature and wind speed and is calculated according to formula (24) [19].

Table 4: Thermal ruler of ASHRAE corresponding to PMV value.

Thermal sensation	Cold	Cool	Coolness	Moderation	Microwarm	Warm	Hot
PMV	−3	−2	−1	0	+1	+2	+2

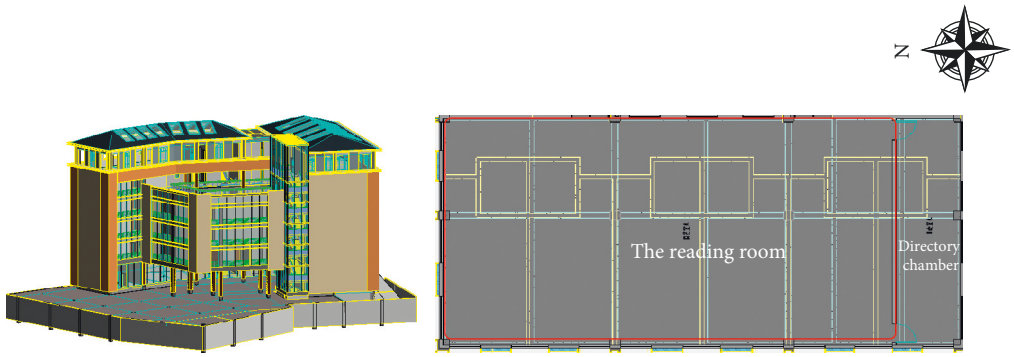

Figure 3: 3D view of the library and reading room plan.

$$f_{\mathrm{cl}} = \begin{cases} 1.00 + 1.29 I_{\mathrm{cl}}, & I_{\mathrm{cl}} \le 0.078, \\ 1.05 + 0.645 I_{cl}, & I_{\mathrm{cl}} > 0.078, \end{cases} \tag{23}$$

$$I_{\mathrm{a}} = \frac{0.155}{\left\{0.61\left((T_i + 273)/298\right)^3 + 1.9\sqrt{v}\,\left(298/\left(T_i + 273\right)\right)\right\}}. \tag{24}$$

T_{mrt} represents the average surface temperature of the area of j surfaces in a room, and its simplified calculation method is as follows:

$$T_{\mathrm{mrt}} = \frac{\sum_{j=0}^{5} A_j T_{is,j}}{\sum_{j=0}^{5} A_j}. \tag{25}$$

3. Case Study

3.1. Building Information. The proposed library is located in Chengdu, Sichuan province, with the coordinates of 30.67° north latitude and 104.02° east longitude. The building floor is the sixth floor, and the model verification object in this paper is the standard floor. Figure 3 shows the library's 3D model and standard layer. The standard floor consists of a reading room and a catalogue room. The entire area has a length of 21.27 m, a width of 11.9 m, and a height of 4.5 m. The total wall area is 221.4 m^2, the floor area is 253.16 m^2, and the ceiling area is 266.9 m^2. The remaining initial input values are rendered in Table 5. What needs to be noted here is that in this calculation, we calculate Pareto values of 10 times of a day in winter and summer, respectively. Here, the average outdoor temperature in Chengdu is $\widetilde{t_{\mathrm{wn}}} = 2.7$°C on a certain day in winter and $T = 2$ on a certain day in summer.

What needs to be explained here is that the value of constant C_1 is obtained according to the case study in literature [17]. Of course, C_1 can be different values for the general solution of ordinary differentiation. When the indoor temperature is 26°C, we calculated the value of C_1 for the verification of this model. In order to simplify the calculation, this paper assumes that the windows are integral and ignores the influence of different window positions on indoor lighting. We have set a total of 625 lighting calculation points in the room, as shown in Figure 4.

Table 5: The remaining initial input data.

Initial input data	
$E_{\mathrm{out},s}$ (lx)	12000
or	0.1
od	0.15
α	1
a_{n} [W/(m²·K)]	8.7
a_w [W/(m²·K)]	23
a_λ	1.2
h_i [W/(m²·K)]	2.2
$\widetilde{T_0}$ (°C)	31
E (W)	534
$M1$ (W/m²)	116
I_{cl} (m²°C/W)	0.0575
C_{p} [kJ/(kg·K)]	0.98
hh	4
R_{k} (m²·K/W)	0.1
C_{m} [kJ/(kg·K)]	1.05
$\widetilde{t_{\mathrm{wn}}}$ (°C)	2.7
Δt_{wn} (°C)	3
h_0 [W/(m²·K)]	5.5
$\Delta\widetilde{T_0}$ (°C)	3
ρ (kg/m³)	1.2
C_1	−2.39
v (m/s)	0.2
T_{sk} (°C)	33.5
Q_{v} (m³/h)	400
C	39

3.2. Data Input. We set a total of 20 design variables, which will provide architects with more abundant energy-saving building design parameters. The value range of these

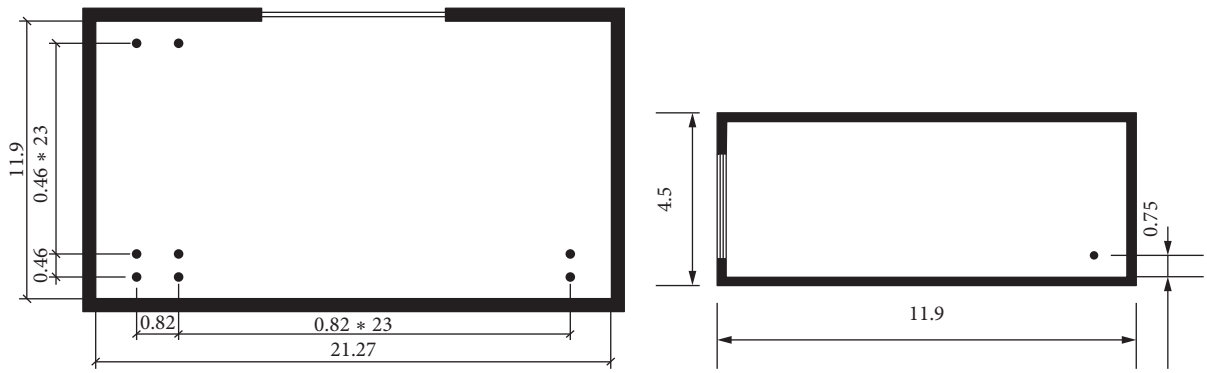

Figure 4: Spatial profile of calculation points (m).

Table 6: The remaining initial input data.

Variable	Symbol	Minimum	Maximum
Window height (m)	H_w	2	4
Window width (m)	L_w	10	18.25
Thickness of concrete (m)	δ_c	0.2	0.3
Thickness of mortar (m)	δ_m	0.02	0.06
The thickness of insulating material (m)	δ_i	0.01	0.06
The thickness of the window pane (m)	w_t	0.003	0.012
Heat transfer coefficient of concrete [W/(m·K)]	λ_c	0.1	1.74
Heat transfer coefficient of the whole window with closed space and window frame area accounting for 20% [W/(m·K)]	λ_w	1.07	5.8
Heat transfer coefficient of concrete	λ_m	0.76	0.93
Heat transfer coefficient of insulating material [W/(m·K)]	λ_i	0.025	0.08
Set indoor temperature in summer (°C)	S_T	24	28
Floor reflection ratio	r_f	0.1	0.5
Wall reflection ratio	r_w	0.3	0.8
The reflection ratio of window glass	r_g	0.07	0.84
Ceiling reflection ratio	r_c	0.6	0.9
The total transmittance of the window	τ_j	0.4	0.84
Density of concrete (kg/m^3)	ρ_c	300	2500
Density of mortar (kg/m^3)	ρ_m	300	1800
The density of insulating material (kg/m^3)	ρ_i	20	180
Set the indoor temperature in winter (°C)	w_T	18	24

variables meets the national design standards [15, 16, 18], as shown in Table 6.

3.3. Method. NSGA-II is based on the evolution of the "individual" group. When the algorithm performs nondominated sorting, each individual in the N-sized population is compared against M objective functions and $N-1$ individuals in the population. NSGA-II needs to save two quantities during sorting:

(i) The number of dominant n_p: this amount is the number of all individuals who can dictate the individual p in the feasible solution space

(ii) The controlled individuals gathered S_p: this quantity is a collection of all individuals in the feasible solution space that is dominated by individual p

In this paper, a total of three objective functions are set, which are in conflict with each other and cannot be compared. It is impossible to obtain the global maximum or minimum like single-objective problems. According to the objective function (fitness function) proposed above, NSGA-II is used to obtain a compromise solution set (nondominant solution) with initial input data and design variables, which does not favour any objective function. Its flow is shown in Figure 5.

The optimizer was drawn up and run by Python 3.7 with a crossover probability of 0.8, a mutation probability of 1/20, an overall size of 100, and a maximum number of iterations of 200 generations.

3.4. Results. It should be reiterated here that f_1 is the total output result of the basic heat consumption of typical

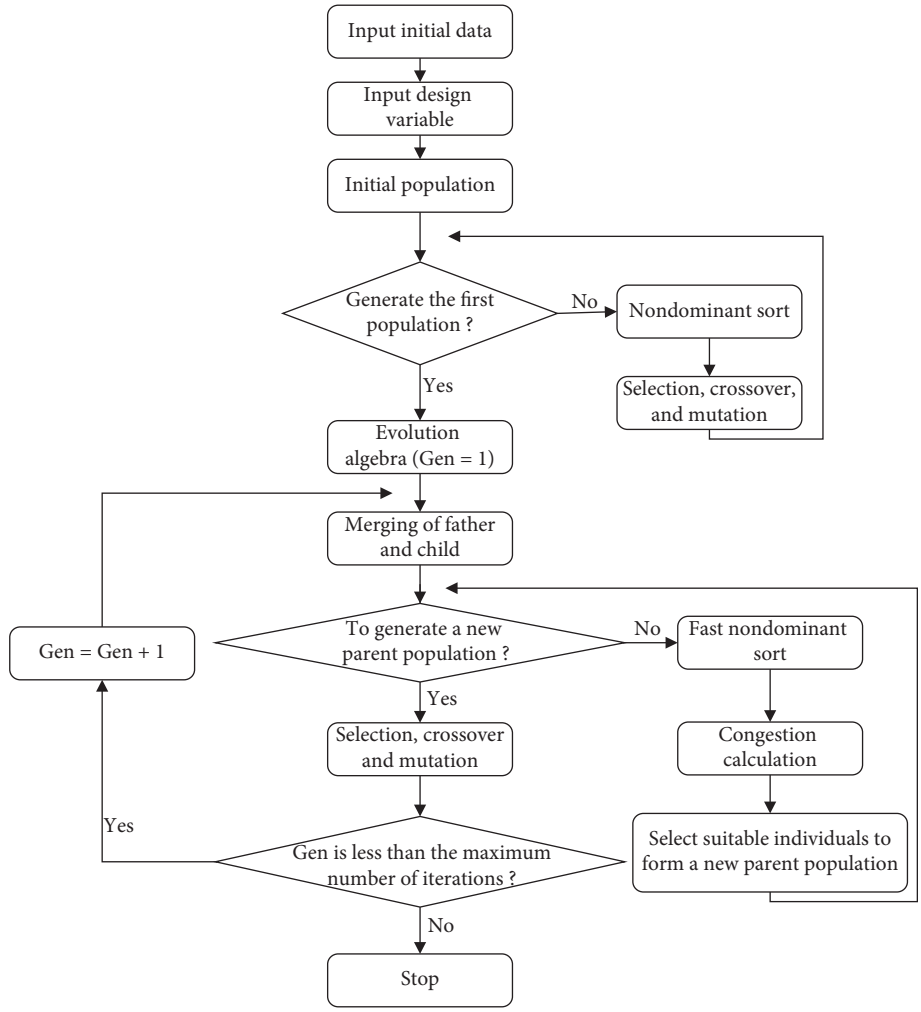

Figure 5: Flowchart of NSGA-II.

climate in Chengdu in winter and the cooling load of typical climate in summer. We calculated 11 moments in winter and summer, respectively. And f_2 represents the annual lighting energy consumption per hour per square meter.

In this process, f_1 and f_2 have a certain coupling, for example, the change of window size will affect the change of f_1 and f_2 output at the same time. Therefore, as f_1 changes in calculation, f_2 will also change correspondingly. In total, we obtained the Pareto solution sets at 11 different moments in a day and the values of corresponding design variables.

According to the calculation result of the above case, for the convenience of the architect to more quickly get detailed building energy efficiency design data, we propose that when two different choices are adopted in the minimum value at 11 moments, the output value of each building parameter is as shown in Tables 7 and 8.

Finally, we give the PMV output results of different selection methods. As can be clearly seen from Figure 6, when f_2 at each moment is selected as the minimum value, the interval of PMV remains at −0.5~0.5. In the other case, all values are higher than 0.5. However, in China, in order to make buildings more energy efficient, the range of PMV is extended to −1~1. Accordingly, these two kinds of choices are to accord with indoor thermal and comfortable requirement. The main reason for this gap is that we only calculate thermal comfort in summer. But, the computational models used are the same in winter and summer. Here, we give more specific design variables of building parameters.

To evaluate the effectiveness of NSGA-II in this article, we use the spacing (SP) [21] method to verify the consistency of the solution set. Firstly, given a solution set $A = \{a_1, a_2, \ldots, a_N\}$,

$$\mathrm{SP}(A) = \sqrt{\frac{1}{N-1}\sum_{i=1}^{N}\left(\overline{d} - d_1\left(a_i, \frac{A}{a_i}\right)\right)^2}, \tag{26}$$

where $\overline{d}$ represents the average of $d_1(a_1, A/a_1)$, $d_1(a_2, A/a_2)$, $\ldots$, $d_1(a_N, A/a_N)$ and $d_1(a_i, A/a_i)$ represents the L^1 norm distance (Manhattan distance) of a_i and established A/a_i.

Table 7: The value of each design variable when f_1 takes the minimum value.

Parameters of the category	The values
The height of the window (m)	3.38
The width of the window (m)	12.48
Thickness of concrete (m)	0.3
Heat transfer coefficient of concrete	0.1
Thickness of mortar (m)	0.06
Heat transfer coefficient of mortar	0.89
The thickness of insulating material (m)	0.06
Heat transfer coefficient of insulating material	0.03
The thickness of the window pane (m)	—
Heat transfer coefficient of window	5.8
Set indoor temperature in summer (°C)	28
The reflection ratio of the floor	0.1
The reflection ratio of the wall	0.3
Window reflection ratio	0.84
Ceiling reflection ratio	0.9
The total transmittance of the window	0.74
Density of concrete (kg/m^3)	1533
Density of mortar (kg/m^3)	1799
Density of insulating material (kg/m^3)	132
Set indoor temperature in winter (°C)	19

Table 8: The value of each design variable when f_2 takes the minimum value.

Parameters of the category	The values
The height of the window (m)	4
The width of the window (m)	17.67
Thickness of concrete (m)	0.2
Heat transfer coefficient of concrete	0.11
Thickness of mortar (m)	0.02
Heat transfer coefficient of mortar	0.76
The thickness of insulating material (m)	0.06
Heat transfer coefficient of insulating material	0.08
The thickness of the window pane (m)	0.012
Heat transfer coefficient of window	5.7
Set indoor temperature in summer (°C)	24
The reflection ratio of the floor	0.5
The reflection ratio of the wall	0.8
Window reflection ratio	0.84
Ceiling reflection ratio	0.9
The total transmittance of the window	0.83
Density of concrete (kg/m^3)	1947
Density of mortar (kg/m^3)	1371
Density of insulating material (kg/m^3)	162
Set indoor temperature in winter (°C)	18

$$d_1(a_i, A/a_i) = \min_{a \in A/a_i} \sum_{j=1}^{m} \left| a_{ij} - a_j \right|, \tag{27}$$

where m represents the number of objectives and a_{ij} represents the solution a_i of the jth objective. When the SP value is close to 0, an excellent consistent solution is obtained. Table 9 shows the SP values at different moments.

From the values of SP at each of the above moments, it can be seen that the solutions at each moment have certain stability. Therefore, we have put forward the most suitable options for architects in the solution set at these moments.

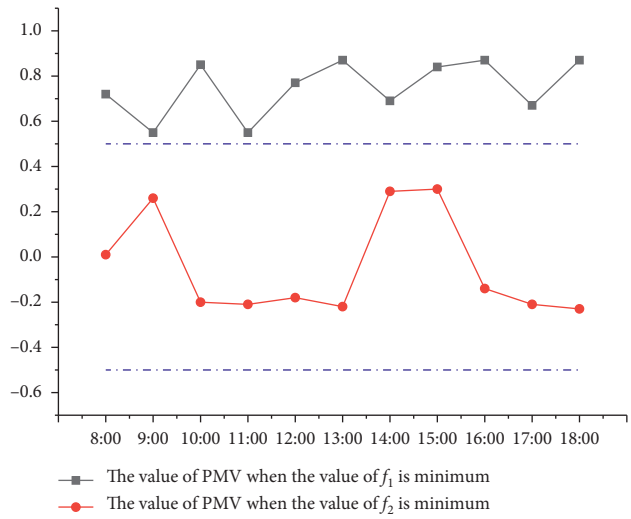

Figure 6: PMV output results of different selections.

Table 9: SP values of solutions at different moments.

Moment	SP
8:00	0.014
10:00	0.067
12:00	0.655
14:00	0.454
16:00	0.665
18:00	0.133
9:00	0.147
11:00	0.011
13:00	0.075
15:00	0.085
17:00	0.624

4. Conclusion and Recommendations for Future Work

This paper introduces a design method of building energy conservation. To implement the model, the nondominant sorting genetic algorithm-II (NSGA-II) is written in the Python environment. In the design questions raised, the design parameters include window size, glass material and specification, floor veneer material, wall veneer material, external wall building material and specification, etc. In addition, the three objective functions of building thermal load, indoor thermal comfort, and lighting energy consumption are considered. Finally, 1100 solution sets are obtained at 11 different moments. In these solution sets, we choose two representative solution sets, which are, respectively, based on the minimum value of building cooling and heating load and the minimum value of lighting energy consumption.

NSGA-II has certain limitations. At present, in the research of energy-saving optimization, many scholars still use NSGA-II to solve three target problems and get excellent results [22–24]. It has developed for nearly 20 years, and the established objective functions are basically no more than three. Due to the proportion of nondominated individuals in the population will rise of power series with the increase of the target space

dimension [25]. Therefore, we will adopt more efficient methods to address optimization problems in future studies.

The construction plan set out in the present paper does not mean specific cost analysis because cost analysis involves the impact of labour costs, construction technology, and local material price fluctuations. Identifiable cost issues can be further analysed on a case-by-case basis. Finally, the contradiction between building energy consumption and indoor environment is closely related to related climate characteristics and renewable energy. We will continue to explore the application and benefits of renewable energy in energy-efficient buildings in the next study.

Nomenclature

H_h: Facade height with window
Q: Heat consumption
E_{el}: Total annual lighting consumption
q_{sys}: Cooling load
τ_j: The glazing transmittance
A_j: Window area
A: The total room surface area
R: The area-weighted mean surface of the room
α: Temperature difference correction factor
F: The area of the envelope
K: Summation heat transfer coefficient
t_n: Heating interior design temperature
t_{wn}: Outdoor design temperature for heating
a_n: Heat transfer coefficient of inner surface of envelope
Δt_{wn}: Outdoor temperature fluctuation range in winter
ω: The angular frequency
or: Orientation correction rate
wp: The wind attachment rate
hh: The external door attachment rate
od: The height addition rate of the building
ir: The intermittent addition rate
Q_v: Ventilation rate
M: Weight of the envelope
ρ: Density
T_{sk}: Mean skin temperature
T_{op}: Operating temperature
I_{cl}: Clothing thermal resistance
I_a: The air thermal resistance
H_w: Window height
L_w: Window width
δ_c: Thickness of concrete
δ_m: Thickness of mortar
δ_i: The thickness of insulating material
w_t: The thickness of the window pane
C_p: The heat capacity of the air
ρ_m: Density of mortar
ρ_i: The density of insulating material
w_T: Set the indoor temperature in winter
ρ_c: Density of concrete
R_{cw}: The area-weighted mean reflectance of the ceiling and walls above the midheight of the window excluding the window wall
L_l: Facade width with window
C: A coefficient depending on the obstruction angle
R_{fw}: The area-weighted mean reflectance of the floor and walls below the midheight of the window excluding the window wall
R_{cw}: The area-weighted mean reflectance of the ceiling and walls above the midheight of the window excluding the window wall
L_i: The length of the window pane
D: The vertical distance between the observation point and the window
E_{in}: The illuminance
E_{out}: The outdoor diffuse illuminance
Q_0: The envelope basically consumes heat
δ: The thickness of the material
a_λ: Correction coefficient of material thermal conductivity
λ: Thermal conductivity of each layer of envelope
R_k: Thermal resistance of closed space layer
a_w: Heat transfer coefficient of outer surface of envelope
$\widetilde{t}_{wn}$: Average calculated outdoor temperature in winter
C_m: The heat capacity of the envelope
T_{is}: Inner surface temperature of the enclosure
h_0: The convective coefficient between the external material and the external air
A_0: Area of external wall
T_0: Outdoor air temperature in summer
h_i: Convection coefficient between the envelope and the indoor air
E: The indoor heat source
$\widetilde{T}_0$: Average outdoor air temperature in summer
$\Delta\widetilde{T}_0$: Outdoor temperature fluctuation range in summer
f_{cl}: Garment area coefficient
HB: Thermal equilibrium coefficient
$M1$: Metabolic rate
T_{mrt}: Mean radiation temperature
λ_c: Heat transfer coefficient of concrete
λ_w: Heat transfer coefficient of the whole window with closed space and window frame area accounting for 20%
λ_m: Heat transfer coefficient of concrete
λ_i: Heat transfer coefficient of insulating material
S_T: Set indoor temperature in summer
r_f: Floor reflection ratio
r_w: Wall reflection ratio
r_g: The reflection ratio of window glass
r_c: Ceiling reflection ratio
τ_j: The total transmittance of the window
R_{fw}: The area-weighted mean reflectance of the floor and walls below the midheight of the window excluding the window wall
C: A coefficient depending on the obstruction angle.

Data Availability

The data used to support the findings of this study are included within the article.

Conflicts of Interest

The authors declare no conflicts of interest.

Acknowledgments

This research is partially supported by the Youth Foundation for Humanities and Social Sciences of Ministry of Education of China (no. 19YJC630063) and the Youth Project of Education Department of Sichuan Province (no. 17ZB0335).

References

[1] International Energy Agency, *2017 Market Report*, International Energy Agency, Paris, France, 2017.

[2] L. Boqiang and L. Hongxun, "China's building energy efficiency and urbanization," *Energy and Buildings*, vol. 86, pp. 356–365, 2015.

[3] P. Jiang, "Analysis of national and local energy-efficiency design standards in the public building sector in China," *Energy for Sustainable Development*, vol. 15, no. 4, pp. 443–450, 2011.

[4] R. Yao, K. Steemers, and B. Li, "Introduction to sustainable urban and architectural design," in *Introduction to Sustainable Urban and Architectural Design*, pp. 1–272, China Architecture and Building Press, Beijing, China, 2006.

[5] P. Heiselberg, H. Brohus, A. Hesselholt, H. Rasmussen, E. Seinre, and S. Thomas, "Application of sensitivity analysis in design of sustainable buildings," *Renewable Energy*, vol. 34, no. 9, pp. 2030–2036, 2009.

[6] S. Gou, V. M. Nik, J.-L. Scartezzini, Q. Zhao, and Z. Lia, "Passive design optimization of newly-built residential buildings in Shanghai for improving indoor thermal comfort while reducing building energy demand," *Energy and Buildings*, vol. 169, pp. 484–506, 2018.

[7] R. Sullivan, D. Arasteh, K. Papamichael et al., "An indices approach for evaluating the performance of fenestration systems in nonresidential buildings," in *Proceedings of the ASHRAE Annual Meeting*, vol. 94, ASHRAE Transactions, Ottowa, Canada, June 1988.

[8] F. Kheiri, "A review on optimization methods applied in energy-efficient building geometry and envelope design," *Renewable and Sustainable Energy Reviews*, vol. 92, pp. 897–920, 2018.

[9] B. Calcagni and M. Paroncini, "Daylight factor prediction in atria building designs," *Solar Energy*, vol. 76, no. 6, pp. 669–682, 2004.

[10] P. R. Tregenza, "Modification of the split-flux formulae for mean daylight factor and internal reflected component with large external obstructions," *Lighting Research and Technology*, vol. 21, no. 3, pp. 125–128, 1989.

[11] A. L. S. Chan, *Methods for Daylight Factor Estimation*, City University of Hong Kong, Hong Kong, 2008.

[12] S. V. Szokolay, *Introduction to Architectural Science: The Basis of Sustainable Design*, Architectural Press, Oxford, UK, 2008.

[13] R. A. Mangkuto and M. A. A. Siregar, "Verification tests of a mirror box type artificial sky without and with building scale model," *Frontiers of Architectural Research*, vol. 7, no. 2, pp. 151–166, 2018.

[14] R. A. Mangkuto, M. A. A. Siregar, A. Handina, and Faridah, "Determination of appropriate metrics for indicating indoor daylight availability and lighting energy demand using genetic algorithm," *Solar Energy*, vol. 170, pp. 1074–1086, 2018.

[15] GB 50034-2013, *Standard for Lighting Design of Buildings*, China Architecture & Building Press, Beijing, China, 2013.

[16] GB 50736-2012, *Design Code of Heating Ventilation and air Conditioning of Civil Buildings*, China Architecture & Building Press, Beijing, China, 2012.

[17] M. Qing, *Research on Using Energy Optimization of Air-Conditioning System in Office Buildings*, Shandong University, Jinan, China, 2012.

[18] GB 50176-2016, *Code for Thermal Design of Civil Building*, China Architecture & Building Press, Beijing, China, 2016.

[19] Y. Hai and W. Runbo, "A simple method for objective evaluation of thermal environment," *Chinese Journal of Ergonomics*, vol. 10, pp. 16–19, 2004.

[20] ISO 7730, "Moderate thermal environment determination of the PMV and PDD indices and specification of the conditions for thermal comfort," International Organization for Standardization, Geneva, Switzerland, 1994.

[21] J. R. Schott, "Fault tolerant design using single and multicriteria genetic algorithm optimization," Master's thesis, Department of Aeronautics and Astronautics, Massachusetts Institute of Technology, Cambridge, MA, USA, 1995.

[22] Y. Zhai, Y. Wang, Y. Huang, and X. Meng, "A multi-objective optimization methodology for window design considering energy consumption, thermal environment and visual performance," *Renewable Energy*, vol. 134, pp. 1190–1199, 2019.

[23] F. Harkouss, F. Fardoun, and P. H. Biwole, "Multi-objective optimization methodology for net zero energy buildings," *Journal of Building Engineering*, vol. 16, pp. 57–71, 2018.

[24] A. Zhang, R. Bokel, A. van den Dobbelsteen, Y. Sun, Q. Huang, and Q. Zhang, "Optimization of thermal and daylight performance of school buildings based on a multi-objective genetic algorithm in the cold climate of China," *Energy and Buildings*, vol. 139, pp. 371–384, 2017.

[25] Z. Juan, "Research on the method of many-objective optimization and the evaluation about redundancy of the objective," Xiangtan University, Xiangtan, Hunan, China, 2014.